Available online at www.sciencedirect.com
SCIENCE DIRECT®
Journal of Power Sources 130 (2004) 15–21
JOURNAL OF POWER SOURCES
www.elsevier.com/locate/jpowsour

Synthesis, sintering and impedance spectroscopy of 8 mol% yttria-doped ceria solid electrolyte

S.K. Tadokoro, T.C. Porfírio, R. Muccillo, E.N.S. Muccillo*

Centro Multidisciplinar para o Desenvolvimento de Materiais Cerâmicos, CCTM, Instituto de Pesquisas Energéticas e Nucleares, C.P. 11.049, Pinheiros, 05422-970 Sao Paulo, SP, Brazil

Received 3 November 2003; accepted 30 November 2003

Abstract

CeO_2–8 mol% Y_2O_3 solid solution was prepared by the coprecipitation technique. Cerium nitrate and yttrium oxide were used as precursors. The main purpose of this work was to evaluate some precipitation parameters, the densification behaviour of powder compacts, and the electrical resistivity of sintered ceramics. Results on thermal analyses show that the decomposition of the precipitated gel is almost complete at 400 °C. The specific surface area of calcined powders decreases for increasing precipitation temperature. For powders precipitated at room temperature, the BET surface area is also found to be dependent on the gel storage time before calcination. The densification of powder compacts increases sharply for sintering temperatures higher than 1400 °C. However, a few minutes at 1500 °C is sufficient for the compacts to attain a high densification. Impedance spectroscopy experiments reveal that the ionic resistivity is not dependent on most of the synthesis parameters, although the grain size play a key role in the intergranular component of the resistivity.

Keywords: Powder synthesis; Ceria; Solid oxide fuel cell; Impedance spectroscopy

1. Introduction

Oxides of the fluorite structure, when doped with divalent or trivalent cations, are good oxygen-ion conductors at high temperatures, and therefore have been of interest in high temperature fuel cells [1,2]. Yttria-stabilised zirconia (YSZ) is the most developed solid electrolyte for solid oxide fuel cell (SOFC) applications. Doped ceria exhibits ionic conductivity values similar to YSZ, but at a lower temperature. Recent experiments have shown that doped ceria may be used as a solid electrolyte for SOFCs in the temperature range of 500–700 °C [3–5].

Highest values for electrical conduction have been obtained with Sm, Gd, and Y as dopants in ceria ceramics [2,6]. Considering the relative abundance of these rare earth elements, yttria-doped ceria is a low-cost alternative for the electrolyte component in SOFCs [7].

The thermal decomposition of metal oxalates have been extensively used for the preparation of mixed oxides and solid solutions at low temperatures [8]. In a number of studies, yttria-doped ceria powders were prepared by the oxalate coprecipitation route [9–13]. Although the influence of the synthesis parameters on the physical properties of the product material had been recognised in these works, additional studies are necessary to obtain a better understand on the role of these parameters on structural characteristics and sintering behaviour of this solid electrolyte material. Moreover, the ionic resistivity of doped ceria depends on the processing parameters, since they determine the values of average grain size and the structure and composition of grain boundaries [14–16].

In this work, CeO_2–8 mol% Y_2O_3 solid solution was prepared by the coprecipitation technique. Some physical properties of powder and compacts have been compared with those of previous works. The main purpose, in this case, was to evaluate the influence of some synthesis parameters on the densification behaviour of ceria–8 mol% yttria powders and on the resulting electrical resistivity of sintered specimens. Therefore, this study has direct relevance to technological applications of this ceramic material.

2. Experimental procedure

2.1. Powder and specimens preparation

$Ce(NO_3)_3{\cdot}6H_2O$ (99.9% Strem Chemicals and 99.999% Aldrich) and Y_2O_3 (99.99% Sigma Chemicals) were used as

* Corresponding author. Tel.: +55-11-3816-9343; fax: +55-11-3816-9370.
E-mail address: enavarro@usp.br (E.N.S. Muccillo).

0378-7753/$ – see front matter © 2003 Elsevier B.V. All rights reserved.
doi:10.1016/j.jpowsour.2003.11.073

starting materials. Other reagents were of analytical grade. A stock yttrium nitrate solution was prepared by addition of hot nitric acid to yttrium oxide. A cerium nitrate stock solution was prepared by dissolution of the precursor material in deionized water. The concentration of these solutions were monitored by gravimetry. For the synthesis of the solid solutions containing 8 mol% yttria, the oxalate coprecipitation technique followed by azeotropic distillation was used. This composition was selected because it gives the highest electrical conductivity value for this solid solution at temperatures of about 700 °C [17].

The precipitation pH was kept constant and equal to 6.5 to ensure a quantitative coprecipitation. The digestion of the precipitate was carried out for 15 min under stirring. The washing of the precipitate was first performed with water, followed by ethanol and isopropanol washings. After partial dehydration, the gel was distilled using *n*-butyl alcohol. The synthesis parameters studied were the precipitation temperature, and the storage time (t_s) at a fixed temperature of 45 °C before characterisation. Further details on the precipitation steps may be found elsewhere [18].

Thermal decomposition of dried gels was carried out at a temperature chosen from thermal analysis results. Disc-shaped specimens were prepared from calcined powders by uniaxial pressing in a stainless steel die at 98 MPa.

2.2. Characterisation of samples

The decomposition behaviour of the dried precipitate was monitored by simultaneous (TG and DTA) thermal analyses (STA 409, Netzsch) up to 1000 °C with a heating rate of 5 °C min^{-1} in synthetic air (∼20% O_2), and using alumina (Alumalox, Alcoa) as reference material. Specific surface area values were determined by nitrogen adsorption/desorption (ASAP 2010, Micromeritics) using the BET (Brunauer, Emmett and Teller) method after degassing calcined powders at 250 °C. X-ray diffraction patterns were obtained on powders and sintered pellets (D8 Advance, Bruker-AXS) using a Ni-filtered Cu Kα radiation in the 20–80° 2θ range for phase analysis. The crystallite size, d_{XRD}, was estimated by the Scherrer equation [19] using Si powder as standard. Average values of crystallite size reported here were calculated from the half-width of the (1 1 1) diffraction peak. In addition, similar calculations were performed for (2 2 0) and (4 2 2) reflections, because they are also sometimes used for that purpose. Differences in the crystallite size lower than 20% were obtained in these cases. Apparent sintered density values were determined by the water immersion technique. A theoretical value of 6.79 g cm^{-3} was assumed [12] for the studied composition.

Some microstructural features were observed on polished and thermally etched surfaces by scanning electron microscopy, SEM (XL30, Philips).

Impedance spectroscopy (HP4192A) measurements were carried out on sintered specimens in the 5 Hz–13 MHz frequency range with an applied ac signal of 50 mV. Silver was used as electrode material. Data were analysed in the impedance mode using a special computer program [20]. Results of electrical measurements are plotted as the imaginary ($-Z''$) versus the real (Z') part of the impedance, normalised for sample dimensions. No corrections for specimens porosity was carried out. The electrical resistivity, ρ, was then calculated from the measured resistances allowing for obtaining Arrhenius plots according to: $\rho = \rho_0 \exp(E/kT)$, where E is the apparent activation energy for the process, k the Boltzmann constant, T the absolute temperature, and ρ_0 the pre-exponential factor.

In the temperature range (200–400 °C) of measurements, impedance diagrams show two semicircles related to the electrical response of the electrolyte material. The high-frequency semicircle is due to the resistive and capacitive effects of the bulk (intragranular response), whereas the low-frequency semicircle is related to the blocking of charge carriers at grain-to-grain interfaces (intergranular response).

3. Results and discussion

Fig. 1 shows thermal analysis results of the precipitated gel after drying for 5 days at 45 °C. The total weight loss was about 46%. The theoretical weight loss (38.2–54%) depends on the degree of hydration of the precipitate. Most of weight loss occurs up to 400 °C and is negligible beyond this temperature. The differential thermal analysis curve shows an exothermic peak centred at 330 °C. This broad exotherm is composed of a peak at 320 °C due to the oxalate decomposition with evolution of CO and CO_2, and another peak at 350 °C assigned to the crystallisation of the solid solution [21]. It is known from the literature [22] that the decomposition temperatures for cerium and yttrium oxalates are 350 and ∼600 °C, respectively. The absence of any thermal event in Fig. 1 for temperatures higher than 350 °C suggests that the solid solution is formed during the precipitation step. Similar results were found by other researchers [11,12].

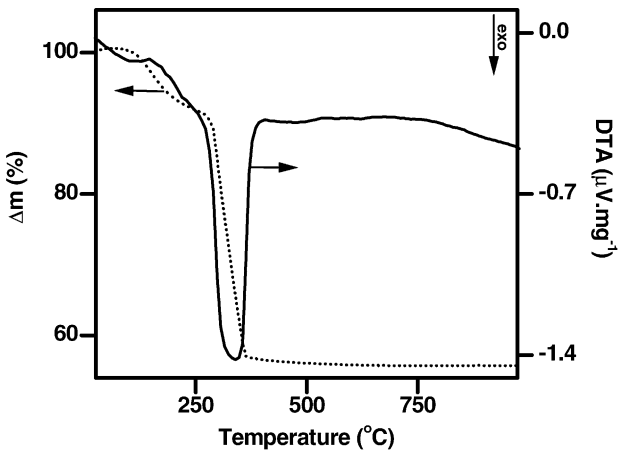

Fig. 1. Thermogravimetric and differential thermal analysis curves of coprecipitated gel.

Table 1
Values of specific surface area, S, and crystallite size, t_{XRD}, obtained for different precipitation temperatures, T_{ppt}

Reference	T_{ppt} (°C)	T_c (°C)	S ($m^2\,g^{-1}$)	t_{XRD} (nm)
This work	25	400	110 (5 days)	5.8
This work	25	400	80 (10 days)	6.0
This work	10	400	104	–
This work	45	400	75	–
[11]	RT	600	14.4	62.0
[13]	RT	500	–	6.0
[12]	RT	500	–	10.0

RT: room temperature; T_c: calcination temperature. The storage time at 45 °C is indicated in parenthesis.

Thermal analysis results for the precipitated gel dried for 10 days at 45 °C are similar to those shown in Fig. 1.

The main differences concerning the precipitation temperature and the storage time are related to the specific surface area determined after calcination at 400 °C. Values of specific surface area are shown in Table 1. Increasing the precipitation temperature to 45 °C, there is a decrease in the specific surface area value. However, for a precipitation temperature of 10 °C, the variation in this parameter is small. A decrease of the specific surface area is also observed for increasing t_s, probably due to the elimination of microporosity. However, the crystallite size does not change significantly with this parameter (Table 1).

It is worth noting that in most cases, calcined powders prepared by this soft chemistry route are formed by nanocrystals (diameter <10 nm). The only exception found in the recent literature is that of precipitates not washed with some organic liquid [11]. This suggests that the mechanism of crystal growth in doped ceria may be governed by surface phenomena provided the interaction between the washing medium and ceria particles is mainly superficial.

X-ray diffraction patterns of powder materials and sintered pellet are shown in Fig. 2. The dried precipitate is amorphous to the X-rays in contrast to previous result where the precipitate had been washed with water [11]. The amorphous character of the precipitate is probably a consequence of the small size of the crystals. This result may be an additional indication that the crystallite growth was inhibited by washing the precipitate in alcoholic medium. After calcination at 400 °C and sintering the diffraction patterns of ceria–yttria samples are essentially unchanged with that of pure ceria (ICDD 34-394). The diffraction peaks became sharp after sintering, indicating high crystallisation and increase of the crystallite size. After sintering at 1400 °C for 6 h, for example, the crystallite size was 72 nm.

Sintering experiments were carried out on compacts prepared with powders precipitated at room temperature and with different storage times. No quantitative differences were observed concerning the influence of this parameter on the sintering behaviour.

Fig. 3 shows the evolution of the relative density with the sintering temperature for a fixed soaking time of 1 h. Specimens were prepared from low purity (99.9%) cerium precursor. The density of compacts remains low up to 1400 °C, but increases sharply for temperatures higher than 1400 °C. This result corroborates most of the available literature data (see, for example, Table 1 in Ref. [10]), and is a consequence of the low sinterability of ceria to which dopants act also as densifier materials.

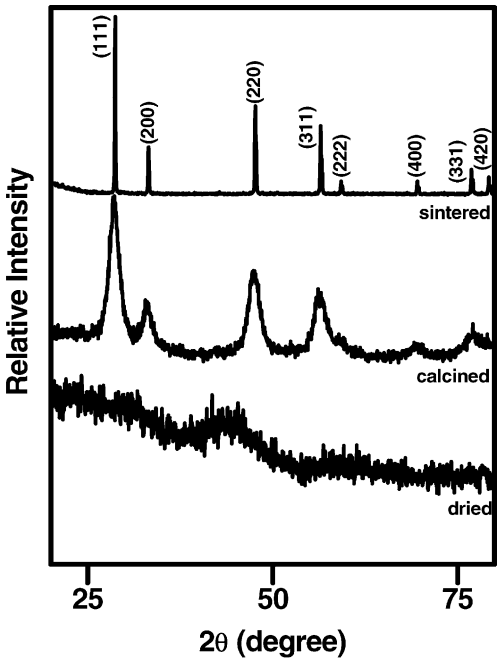

Fig. 2. X-ray diffraction patterns of ceria–yttria powders.

Fig. 4 shows SEM micrographs of specimens sintered for 1 h at 1400 °C (Fig. 4a) and 1500 °C (Fig. 4b). Sintering at 1400°C resulted in a sub-micrometer grain size. In addition, grains are uniform in size and shape, and there is no evidence of exaggerated grain growth. For the specimen sintered at 1500 °C negligible porosity is observed, and grains have grown by a factor of approximately 4 compared to specimens sintered a 1400 °C.

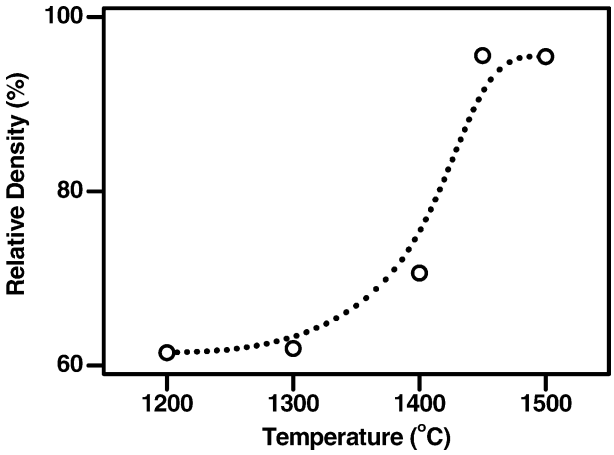

Fig. 3. Dependence of the relative density of powder compacts on the sintering temperature.

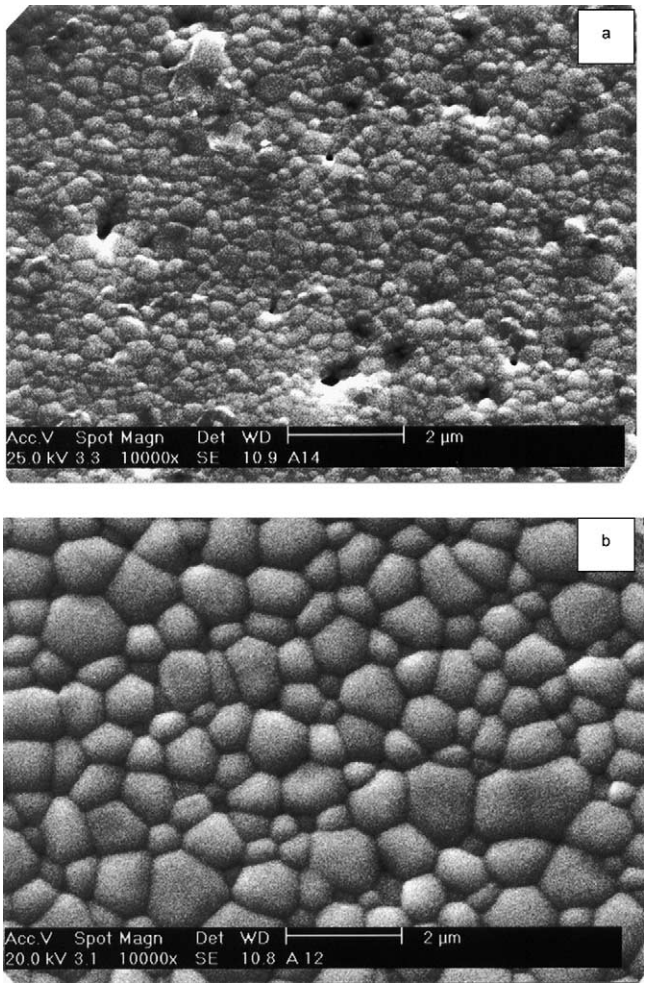

Fig. 4. SEM micrographs of pellets sintered for 1 h at 1400 °C (a) and 1500 °C (b).

Impedance diagrams of specimens sintered at 1300, 1400 and 1500 °C for 1 h are shown in Fig. 5. These diagrams were obtained at a measuring temperature of 234 °C. For the sake of clarity, only the high-frequency part of diagrams was plotted. Numbers in these and other diagrams represent the logarithm of the frequency, in Hz. These diagrams reveal a decrease in the electrical resistivity of the bulk material with increasing the sintering temperature. The relative magnitude of this behaviour is better seen in the Arrhenius plots of Fig. 6a. The difference in the bulk resistivity between specimens sintered at 1200 and 1500 °C is less than one order of magnitude for a fixed temperature of measurement. In addition, there is no net variation of the intragranular resistivity after sintering at and above 1450 °C. Considering that the solid solution was formed during the coprecipitation step, and taking into account that yttrium segregation may be occurred at some extent, this difference in electrical resistivity should be related to a better solubilisation and homogenisation of the solute in the ceria matrix with the increase of the sintering temperature. In effect, solute segregation at grain boundaries was demonstrated to occur in fluorite-structured ceramics [23,24]. The important point here is the existence of a minimum sintering temperature to attain a lower bulk resistivity.

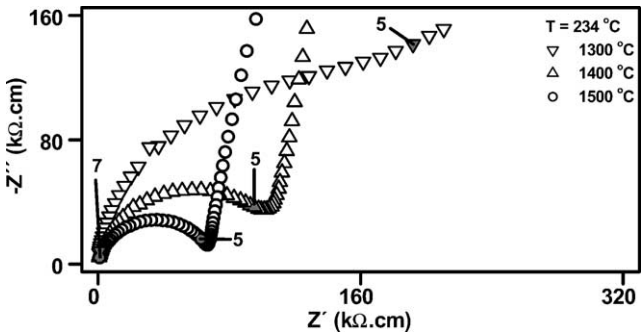

Fig. 5. High-frequency part of impedance diagrams of pellets sintered at different temperatures for 1 h. Measuring temperature = 234 °C.

The Arrhenius plots of the intergranular component of the electrical resistivity for specimens sintered for 1 h at different temperatures is shown in Fig. 6b. A similar behaviour to that of the intragranular resistivity is seen, that is, the resistivity decreases with increasing the sintering temperature. In this case, however, the difference between the resistivity of specimens sintered at 1200 and 1500 °C, for a fixed measuring temperature, is higher than one order of magnitude. The main reasons for this difference

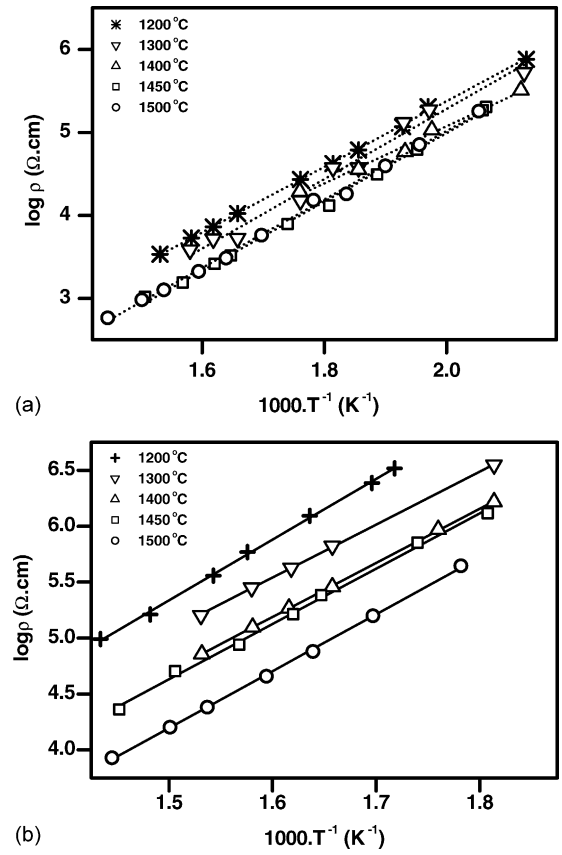

Fig. 6. Arrhenius plots of intragranular (a) and intergranular (b) components of the electrical resistivity of pellets sintered at different temperatures for 1 h.

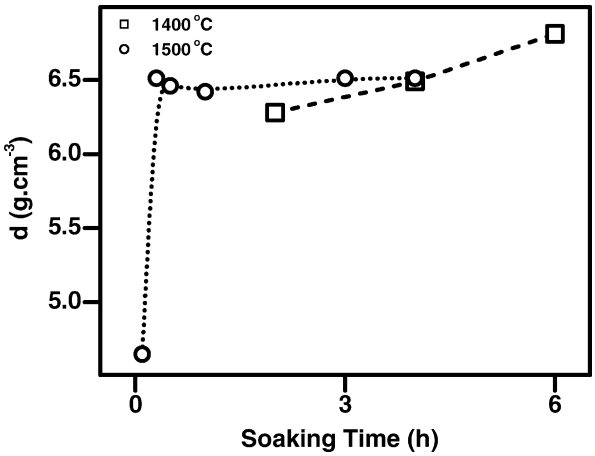

Fig. 7. Dependence of the apparent density on the soaking time for pellets sintered at 1400 and 1500 °C.

are the elimination of interconnected porosity and grain growth. The former should be dominant for sintering temperatures up to 1450 °C, whereas the later predominates for higher temperatures. Hence, comparing results of Figs. 3, 4, and 6b, it is evident that the densification and the consequent reduction in the number of interfaces, and grain growth play a major role for the decrease of the intergranular resistivity.

The densification behaviour with the soaking time at fixed temperatures is shown in Fig. 7. Specimens sintered at 1400 °C exhibit a gradual increase in the relative density up to 6 h. The lowest density (∼93% of the theoretical value) was obtained for a soaking time of 2 h. For a soaking time of 6 h the relative density is approximately 100%. These specimens were prepared from high purity (99.999%) cerium precursor. The above results strongly suggest that for temperatures up to 1400 °C, sintering of ceria–yttria ceramics is dominated by a solid state mechanism with low-pore elimination kinetics. Increasing sintering temperature to 1500 °C, the densification behaviour is different. For a sintering time of 0.1 h the relative density was only 69%, whereas for a soaking time of 0.3 h this value reached 96% and remained approximately constant up to 4 h at that temperature. This observation suggests that at some temperature higher than 1400 °C, another phenomenon may influence the sintering behaviour of ceria–yttria specimens. Considering the relatively low purity (99.9%) of the starting material in this case, the fast densification of specimens at 1500 °C may be attributed to a liquid-phase sintering mechanism operating at this temperature. The presence of a liquid at the sintering temperature enhances mass transfer, densification, and microstructure coarsening [25]. This liquid-phase may be formed by impurities present in the precursor materials. One of the most common impurities in ceria-based ceramics is silicon, which readily forms melted silicate-phases between 800 and 1500 °C. Although the presence of small amounts of SiO_2 in doped ceria is detrimental to the electrical conductivity [26], it enhances the densification during sintering of these ceramic materials.

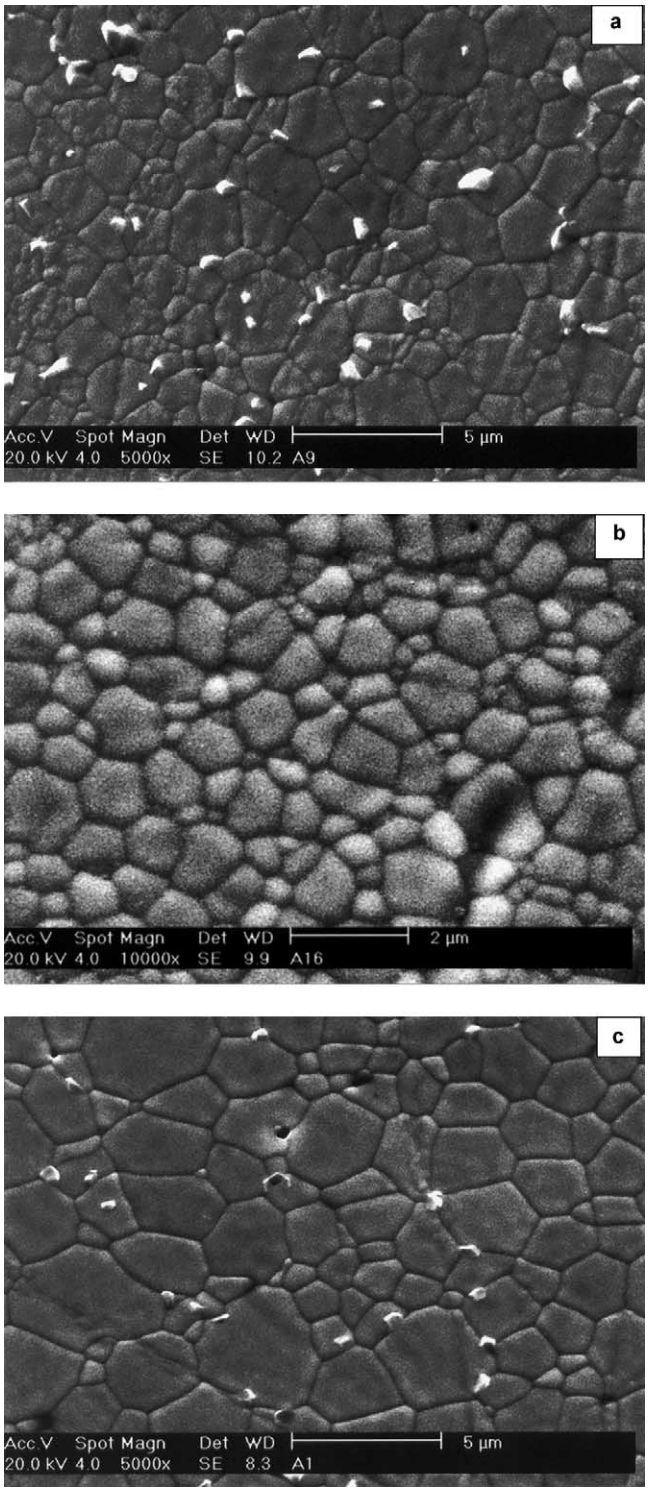

Fig. 8. SEM micrographs of pellets prepared from powders with different degrees of purity sintered at 1500 °C for 4 h (a), 1400 °C for 6 h (b), and 1500 °C for 4 h (c). Purity of precursor material: (a) 99.9%, (b) and (c) 99.999%.

Fig. 8 shows representative SEM micrographs of pellets sintered at 1500 °C for 4 h (a), prepared with low purity precursor, and sintered at 1400 °C for 6 h (b) and 1500 °C for 4 h (c), prepared with high purity precursor. The

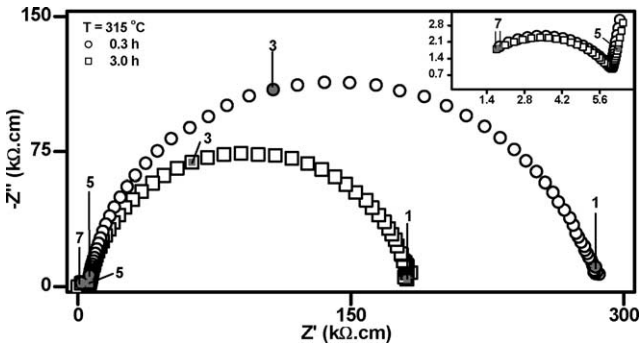

Fig. 9. Impedance diagrams of pellets sintered at 1500 °C for 0.3 and 3 h. Measuring temperature = 315 °C.

microstructure in Fig. 8a reveals a non-uniform distribution of grains with small (<1 μm) and very large (>4 μm) grains.

Specimens prepared with high purity precursor and sintered at 1400 °C for 6 h (Fig. 8b) and 1500 °C for 4 h (Fig. 8c) also show a non-homogeneous distribution of grain sizes. However, the difference between the sizes of smaller and larger grains is lower, and grains are more angular. A more detailed analysis on the effect of the precursor purity on electrical conductivity of yttria-doped ceria will be published elsewhere [27].

Typical impedance diagrams for pellets sintered at 1500 °C are shown in Fig. 9 for soaking times of 0.3 and 3 h. As expected, the intragranular component of the electrolyte resistivity (see the inset) does not experience any change with the soaking time, whereas the intergranular resistivity decreases with increasing soaking time due to the increase in grain size.

Arrhenius plots of intra- and intergranular components of the total resistivity are shown in Fig. 10. As can be seen in these plots, the relative difference in the intergranular resistivity of different specimens is small, indicating that the microstructure of sintered pellets does not change to a significant extent with the soaking time at 1500 °C. Therefore,

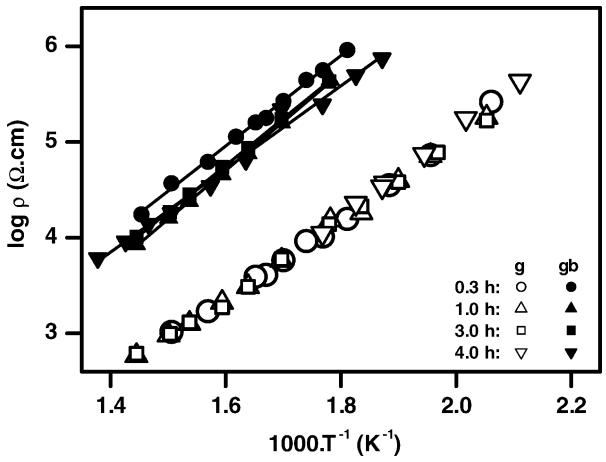

Fig. 10. Arrhenius plots of intra- and intergranular components of the electrical resistivity of pellets sintered at 1500 °C at different soaking times.

for a fixed sintering temperature, grain growth is not of primary importance to change the specimen microstructure, at least in the limited soaking times studied.

Apparent activation energy values for all studied specimens calculated from the slope of the Arrhenius plots are ~0.8 and 0.9 eV for intra- and intergranular components of the resistivity, respectively. The only exception was found for the specimen sintered at 1200 °C for 1 h, which presented a lower value for the intragranular (~0.76 eV) and higher value for the intergranular (~1.05 eV) resistivity. These figures are in general agreement with the literature data.

4. Conclusions

The oxalate coprecipitation chemical processing of yttrium and cerium precursors leads to the production of nanocrystalline (average size <10 nm) powders after calcination at 400 °C. These powders may reach high density values (relative density >95%) after sintering.

The coprecipitation temperature and the storage time at 45 °C was found to influence the specific surface area of calcined powders.

Full density could be obtained for pellets prepared from high purity precursor material by sintering at 1400 °C. In contrast, specimens prepared from low purity precursor did not attain full densification, even after sintering at higher temperature (1500 °C).

The relative homogeneity and grain size of sintered pellets was found to depend on sintering conditions and also on the purity of the precursor material. These factors are proposed here to control the sintering mechanism and the electrical resistivity of this solid solution.

Acknowledgements

To FAPESP (99/04929-5, 96/09604-9 and 95/05175-4) that sponsored most of the facilities used in this work. To CNPq (300934/94-7), CNEN and PRONEX. T.C. Porfírio thanks to FAPESP (00/11417-0) for the scholarship.

References

[1] N.Q. Minh, J. Am. Ceram. Soc. 76 (1993) 653.
[2] H. Inaba, H. Tagawa, Solid State Ionics 83 (1996) 1.
[3] G.M. Christie, F.P.F. Van Berkel, Solid State Ionics 83 (1996) 17.
[4] B.C.H. Steele, Solid State Ionics 129 (2000) 95.
[5] R. Doshi, V.L. Richards, J.D. Carter, X. Wang, M. Krumpelt, J. Electrochem. Soc. 146 (1999) 1273.
[6] H. Yahiro, Y. Baba, K. Eguchi, H. Arai, J. Electrochem. Soc. 135 (1988) 2077.
[7] J. Van Herle, T. Horita, T. Kawada, N. Sakai, H. Yokokawa, M. Dokiya, Solid State Ionics 86–88 (1996) 1255.
[8] J. Robin, Bull. Soc. Chim. Fr. 20 (1953) 1078.
[9] K. El Adham, A. Hammou, J. Chim. Phys. Phys.-Chim. Biol. 79 (1982) 633.

[10] J. Van Herle, T. Horita, T. Kawada, N. Sakai, H. Yokokawa, M. Dokiya, J. Am. Ceram. Soc. 80 (1997) 933.
[11] K. Higashi, K. Sonoda, H. Ono, S. Sameshima, Y. Hirata, J. Mater. Res. 14 (1999) 957.
[12] Y. Gu, G. Li, G. Meng, D. Peng, Mater. Res. Bull. 35 (2000) 297.
[13] S. Zha, Q. Fu, Y. Lang, C. Xia, G. Meng, Mater. Lett. 47 (2001) 351.
[14] I. Riess, D. Braunshtein, D.S. Tannhauser, J. Am. Ceram. Soc. 64 (1981) 479.
[15] S.J. Hong, K. Mehta, A.V. Virkar, J. Electrochem. Soc. 145 (1998) 638.
[16] C.K. Chiang, J.R. Bethin, A.L. Dragoo, A.D. Franklin, K.F. Young, J. Electrochem. Soc. 129 (1982) 2113.
[17] G.B. Balazs, R.S. Glass, Solid State Ionics 76 (1995) 155.
[18] S.K. Tadokoro, E.N.S. Muccillo, J. Eur. Ceram. Soc. 22 (2002) 1723.
[19] B.E. Warren, X-ray Diffraction, Dover, New York, 1990.
[20] M. Kleitz, J.H. Kennedy, in: P. Vashishta, J.N. Mundy, G.K. Shenoy (Eds.), Fast Ion Transport in Solids, Electrodes and Electrolytes, North-Holland, Amsterdam, 1979, p. 185.
[21] R.P. Agarwala, M.C. Naik, Anal. Chim. Acta 24 (1961) 128.
[22] M.J. Fuller, J. Pinkstone, J. Less-Common Met. 70 (1980) 127.
[23] C.Y. Lei, Y. Ito, N.D. Browning, J. Am. Ceram. Soc. 85 (2002) 2359.
[24] Y.-M. Chiang, E.B. Lavik, D.A. Blom, Nanostruct. Mater. 9 (1997) 633.
[25] R.M. German, Sintering Theory and Practice, Wiley/Interscience, New York, 1996.
[26] T.S. Zhang, J. Ma, L.B. Kong, P. Hing, Y.J. Leng, S.H. Chan, J.A. Kilner, J. Power Sources 124 (2003) 26–33.
[27] S.K. Tadokoro, E.N.S. Muccillo, J. Alloys Compd., in press.